Antigen stored in dendritic cells after macropinocytosis is released unprocessed from late endosomes to target B cells

Delphine Le Roux,[1-3] Agnès Le Bon,[1-3] Audrey Dumas,[1-3] Kahina Taleb,[1-3] Martin Sachse,[4] Romain Sikora,[1-3] Marion Julithe,[1-3] Alexandre Benmerah,[1-3] Georges Bismuth,[1-3] and Florence Niedergang[1-3]

[1]Inserm U1016, Institut Cochin, Paris, France; [2]Centre National de la Recherche Scientifique, Unité Mixte de Recherche 8104, Paris, France; [3]Université Paris Descartes, Sorbonne Paris Cité, Paris, France; and [4]Institut Pasteur-Imagopole, Paris, France

B lymphocytes can be triggered in lymph nodes by nonopsonized antigens (Ag), potentially in their native form. However, the mechanisms that promote encounter of B lymphocytes with unprocessed antigens in lymph nodes are still elusive. We show here that antigens are detected in B cells in the draining lymph nodes of mice injected with live, but not fixed, dendritic cells (DCs) loaded with antigens. This highlights active processes in DCs to promote Ag transfer to B lymphocytes. In addition, antigen-loaded DCs found in the draining lymph node were CD103$^+$. Using 3 different model Ag, we then show that immature DCs efficiently take up Ag by macropinocytosis and store the internalized material in late endocytic compartments. We find that DCs have a unique ability to release antigens from these compartments in the extracellular medium, which is controlled by Rab27. B cells take up the regurgitated Ag and the chemokine CXCL13, essential to attract B cells in lymph nodes, enhances this transfer. Our results reveal a unique property of DCs to regurgitate unprocessed Ag that could play an important role in B-cell activation. (*Blood*. 2012; 119(1):95-105)

Introduction

Dendritic cells (DCs) are key players in initiating specific immune responses. They display an extensive capacity for antigen (Ag) uptake in the periphery. After Ag internalization and migration to the draining lymph node, they present antigenic peptides, generated by intracellular Ag processing, to activate naive T cells.[1,2]

In contrast, as B cells recognize Ag in its native, unprocessed form, via their surface immunoglobulin receptor (BCR), the logistics of B-cell antigen presentation and activation in the lymph node is much less clearly defined. Lymphoid tissue architecture limits passive diffusion of large Ag,[3-6] and some Ag-presenting cells have been proposed as Ag carriers in lymph nodes: B cells, DCs, follicular DCs, subcapsular sinus, and medulla macrophages.[7-13] Interestingly, direct interactions of B cells with DCs have been seen in vitro[14] and in vivo.[7,15] This interaction is necessary for isotype switching and production of high affinity antibodies,[16,17] indicating that the dialogue between DCs and B cells is a crucial step in initiating efficient immune response. However, it is still unclear whether in this case Ags are internalized before delivery to B cells.

Macropinocytosis is one way immature DCs use to sample their environment and capture Ag. It is constitutive in immature DCs and down-regulated on DCs maturation. As opposed to other endocytic routes, macropinocytosis does not involve specific receptors, relies on large membrane ruffles to form the macropinosome,[18-21] and involves the small GTP-binding proteins Cdc42, Rac1, and ADP-ribosylation factor 6.[22-25] It has long been known that the way of entry of a given Ag will influence its endocytic route,[26-28] but the intracellular fate of macropinocytosed Ag in DCs is still unclear. Besides their degradation activity, murine DCs have the capacity to store native Ag.[16,26,29,30] This storage property probably represents a pool for later Ag processing, thus allowing sustained presentation to CD4 and CD8 T cells.[31,32] Intradermally injected DCs were found mainly at the boundary between the T- and B-cell zone.[33,34] Because DCs are less degradative than macrophages,[29-31] we hypothesized that they could preserve part of the Ag from the periphery and subsequently deliver it to B cells in the lymph node.

In this study, we show, for the first time, that macropinocytosed Ag was partially released by DCs from late endosomal compartments under its native form in the extracellular medium and taken up by specific B cells. This Ag release was enhanced when DCs were treated with the B-cell chemoattractant, CXCL13. We observed Ag delivery to B cells in vivo in mice after injection of Ag-pulsed DCs but not Ag-pulsed fixed DCs. Loaded DCs found in the lymph node were CD103$^+$. This work provides evidence for a unique pathway of Ag storage and delivery by DCs to B cells and should help us to understand the very first steps of the innate and adaptive immune responses.

Methods

Cells

For generation of human immature DCs, peripheral blood mononuclear cells were isolated from leukapheresis by density-gradient separation on Ficoll-Paque Plus (GE Healthcare; supplemental Methods, available on the *Blood* Web site; see the Supplemental Materials link at the top of the online article).

Human autologous B cells were enriched from leukapheresis blood using a human B-cell enrichment cocktail according to the manufacturer's instructions (RosetteSep; StemCell Technologies) and frozen at −80°C in

Submitted February 12, 2011; accepted October 9, 2011. Prepublished online as *Blood* First Edition paper, November 2, 2011; DOI 10.1182/blood-2011-02-336123.

The online version of this article contains a data supplement.

The publication costs of this article were defrayed in part by page charge payment. Therefore, and solely to indicate this fact, this article is hereby marked "advertisement" in accordance with 18 USC section 1734.

FCS with 10% DMSO until use. B-cell enrichment was assessed each time by flow cytometry and was consistently 90%.

B cells were purified by negative selection from lymph nodes, and murine DCs were purified by positive selection using CD11c$^+$ magnetic microbeads (Miltenyi Biotec) from a mixture of spleen and lymph nodes of C57Bl/6 mice (Harlan).

Footpad injections of purified murine DCs

Purified DCs from C57Bl/6 mice were incubated with 50 mg/mL of QDot655 or 605-coupled F(ab)′$_2$ anti–mouse IgG (Invitrogen) for 1 hour at 37°C. Cells were then washed twice with sterile PBS, and half of them were fixed with 4% paraformaldehyde (PFA, Sigma-Aldrich) for 10 minutes and washed again before footpad injection into C57/Bl6 mice. Five mice of each group were injected in each footpad with 2.5×10^6 pulsed DCs (fixed or not). After 18 hours, cell suspensions were obtained from draining popliteal lymph nodes (PLNs). Cells were stained with allophycocyanin-anti–murine CD11c and PE-anti–murine CD19 antibodies (BD Biosciences) or with PE-Cy7-anti–CD11c, peridinin chlorophyll protein-anti–MHC II, biotin-anti–CD317 (eBioscience), Pacific Blue-anti–CD8α, FITC-anti–CD19, PE-anti–CD103 (BD Biosciences), and streptavidin-allophycocyanin or AlexaFluor-750 (Invitrogen). Samples were analyzed by flow cytometry using the BD LSRII cytometer and BD FACSDiva Version 6.1.2 software (BD Biosciences; Cochin Immunobiology Facility). Results are expressed in numbers of CD11c$^+$/QDot$^+$ and CD19$^+$/QDot$^+$ cells found in the lymph nodes. In addition, PLNs of one mouse of each group were embedded in OCT and stored at −80°C before sectioning (CM350S, Leica); 7-mm sections were fixed in 1% PFA and then washed and blocked with PBS supplemented with 3% BSA. Sections were then stained with PE-anti–CD11c and FITC-anti–CD19 antibodies (BD Bioscience). After washes, sections were covered with glass coverslips using FluoromountG (Interchim).

Image acquisition

For details regarding image acquisition for Figures 1 through 5, please see supplemental Methods.

Results

Monocyte-derived immature DCs internalize antigens by macropinocytosis

We first analyzed the mechanisms of antigen uptake and delivery by DCs in human DCs derived in vitro from monocytes of healthy donors after a 5-day GM-CSF plus IL-4 treatment (MoDCs). Immature CD11c$^+$ CD14$^-$ DCs were harvested at day 5 after purification (supplemental Figure 1A).

To explore the endocytic activity of the MoDCs, both immature and mature MoDCs were incubated with 1 mg/mL of FITC-coupled large dextran (500 kDa), commonly used as a marker of macropinocytosis, as well as with proteins of lower molecular weight, including F(ab)′$_2$ anti–human IgG (100 kDa) or HRP (40 kDa) and another fluid-phase marker, Lucifer Yellow, as a small compound (457 Da). As expected, immature MoDCs internalized 500 kDa dextran in a time-dependent manner without reaching a plateau, even after a 1-hour incubation (Figure 1A). In contrast and as previously reported,[22,23,35] mature MoDCs internalized a very small amount of dextran (Figure 1A). We observed that dextran uptake involved the mannose receptor, as previously described,[35] whereas internalization of Lucifer Yellow or F(ab)′$_2$ did not (supplemental Figure 1B).

To better define the internalization pathway, we pretreated MoDCs with different drugs: cytochalasin D, which blocks actin polymerization, wortmaninn to inhibit PI3K, or amiloride, which inhibits the sodium channels and is important for regulation of intracellular pH and actin polymerization and considered as the most specific drug for macropinocytosis.[19,24] Internalization of dextran, F(ab)′$_2$, and HRP was inhibited in cells treated with these drugs, compared with control conditions (Figure 1B-D), whereas Lucifer Yellow uptake by MoDCs was not impaired in immature MoDCs by these drugs (Figure 1E), indicating that it might enter into DCs by fluid-phase endocytosis.

Finally, we analyzed whether dynamin was required (Figure 1F-G). Dynamin is a large G protein involved in vesicle fission.[36] Expression of wild-type or dominant-negative (K44A mutant) forms of dynamin2 in immature MoDCs did not alter the efficiency of dextran uptake. In addition, cells were treated with dynasore, a specific drug that inhibits both dynamin (1 and 2).[37] Whereas transferrin endocytosis was strongly impaired in dynasore-treated cells as expected, neither dextran nor F(ab)′$_2$ anti–human IgG internalization was affected, indicating that macropinocytosis of dextran and F(ab)′$_2$ by MoDCs does not require dynamin activity.

We then observed the internalized Ag by microscopy. Analysis of deconvolved Z-stack fluorescence microscopy images showed that, after 30 minutes of incubation with different macropinocytosed Ag, cells exhibited endocytic compartments of heterogeneous size scattered throughout the cell body (Figure 1H). None was in the range of several microns, as opposed to the macropinocytic vesicles induced by growth factors.[18] To further characterize the endocytic pathway used by macropinocytosed Ag at the ultrastructural level, cryosections of F(ab)′$_2$-pulsed DCs were immunolabeled for the Ag (Figure 1I). After 1 hour of Ag pulse, the F(ab)′$_2$ was detected in early endosomes but also in dense late-endosome structures, and in tubular elements. Of note, we did not detect the presence of F(ab)′$_2$ at the plasma membrane (Figure 1I).

Taken together, these results indicate that immature MoDCs capture dextran, F(ab)′$_2$ anti–human IgG, and HRP proteins by a PI3K- and actin-dependent, amiloride sensitive, dynamin-independent, macropinocytic process of internalization that does not form large macropinosomes in these cells.

Intracellular fate of macropinocytosed Ag in MoDCs

We next aimed to follow the intracellular fate of macropinocytosed Ags in MoDCs. For this, cells were pulsed with FITC-labeled F(ab)′$_2$ anti–human IgG for one hour and then washed and cultured for different time points before analysis by flow cytometry. F(ab)′$_2$ anti–human IgG was still detected in MoDCs after 4 and 18 hours of chase (Figure 2A). Intracellular localization of macropinocytosed Ag was then analyzed by fluorescence microscopy after 4 hours of chase (Figure 2B-C). Cells were fixed and stained for CD63 and Lamp1. The majority of macropinocytosed Ag reached CD63$^+$ or Lamp1$^+$ late endosomal compartments after 1 hour of pulse, where they could still be detected after 4 hours of chase. Intracellular macropinocytosed Ag was further analyzed by electron microscopy in MoDCs pulsed for 1 hour with F(ab)′$_2$ and then chased for 4 hours without Ag (Figure 2D). Label for the F(ab)′$_2$ was found in electron-dense late endosomal compartments similar to the one observed after 1-hour chase, confirming the Ag storage in late endosomal structures.

Macropinocytosed Ag is released by DCs in the extracellular environment under its native form

We further analyzed the fate of macropinocytosed Ag, with the hypothesis that MoDCs could regurgitate an internal Ag under its native form after macropinocytosis. For this, we designed an assay using HRP, with which the enzymatic activity can be measured in

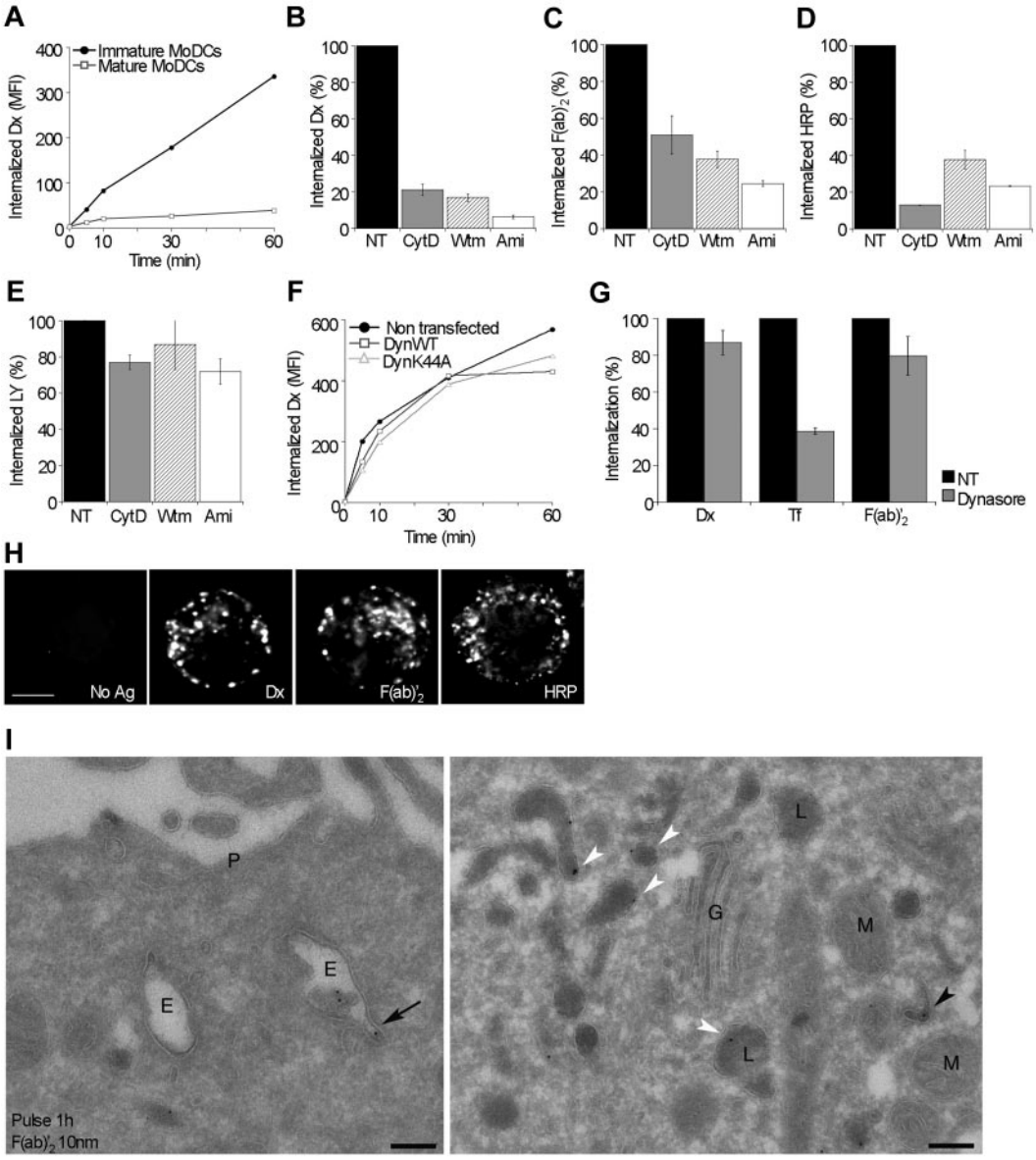

Figure 1. Immature MoDCs internalize Ag by macropinocytosis. (A) Flow cytometric analysis of internalization of fluorescein-coupled 500 kDa dextran by immature versus LPS-matured MoDCs. (B-E) Immature MoDCs were pretreated with cytochalasin D, wortmannin, or amiloride for 30 minutes before addition of dextran (B), F(ab)′$_2$ (C), HRP (D), or Lucifer Yellow (E) for 30 minutes. Cells were analyzed by flow cytometry. Results are expressed as a percentage of control nontreated (NT) cells. Data are mean ± SEM of 3 independent experiments. (F) Immature MoDCs were transfected or not with plasmids encoding the wild-type (DynWT) or the dominant-negative form (DynK44A) of dynamin2 coupled to GFP and then incubated with 500 kDa dextran, followed by flow cytometry. Mean fluorescence intensities (MFI) are plotted. (G) Immature MoDCs were treated or not (NT) with dynasore and incubated with fluorescent dextran, transferrin, or F(ab)′$_2$ for 30 minutes at 37°C. Cells were analyzed by flow cytometry. Results are expressed as a percentage of control nontreated (NT) cells. Data are mean ± SEM of 3 independent experiments. (H) Immature MoDCs were incubated with dextran, F(ab)′$_2$, or HRP for 30 minutes and then fixed and analyzed by wide field microscopy and deconvolution. A medial optical section is shown. Bar represents 5 μm. (I) Immature MoDCs were pulsed for 1 hour with 50 μg/mL F(ab)′$_2$ and then fixed and prepared for electron microscopy after immunogold labeling on thawed cryosections (10 nm-gold particles). The white arrowheads indicate label in late endosomal vacuoles; and black arrowhead, label in a tubular structure. The black arrow points to a label in a tubular extension of an early endosomal vacuole. P indicates plasma membrane; E, early endosomal vacuole; G, Golgi; M, mitochondrium; and L, late endosomal/lysosomal vacuole. Bar represents 200 nm.

cell-associated fractions as well as in supernatants, when it is released in the external medium. MoDCs were pulsed for 1 hour with 1 mg/mL of HRP, then washed and incubated at 37°C for different time points (Figure 3A). Acid-washed and trypsinized MoDCs were analyzed in parallel to remove any HRP bound to the cell surface (Figure 3A). After 1 hour, up to 0.2 μg/mL of HRP was detected in the supernatant of untreated MoDCs, which corresponds to 10% to 30% of internalized HRP. Acid wash or trypsin treatment reduced the amount of HRP present in the supernatant, indicating that some HRP was bound to the cell membrane and could detach. Pretreated cells, however, still released HRP to the extracellular medium with the same slope (Figure 3A). Hence, acid treatment was used in all subsequent experiments. We observed that, despite different Ag uptake capacities, MoDCs from different donors showed the same ability to deliver unprocessed HRP to the extracellular medium up to 6 hours (Figure 3B) and calculated a rate of regurgitation of approximately 20 ng/mL per hour per 10^5 MoDCs. The release of HRP in the medium did not reach a plateau even after 6 hours of chase, indicating that this delivery of HRP in the medium was not saturable. Of note, it is unlikely that the observed HRP release in the supernatant was the result of release from dead cells because the percentage of dead cells we

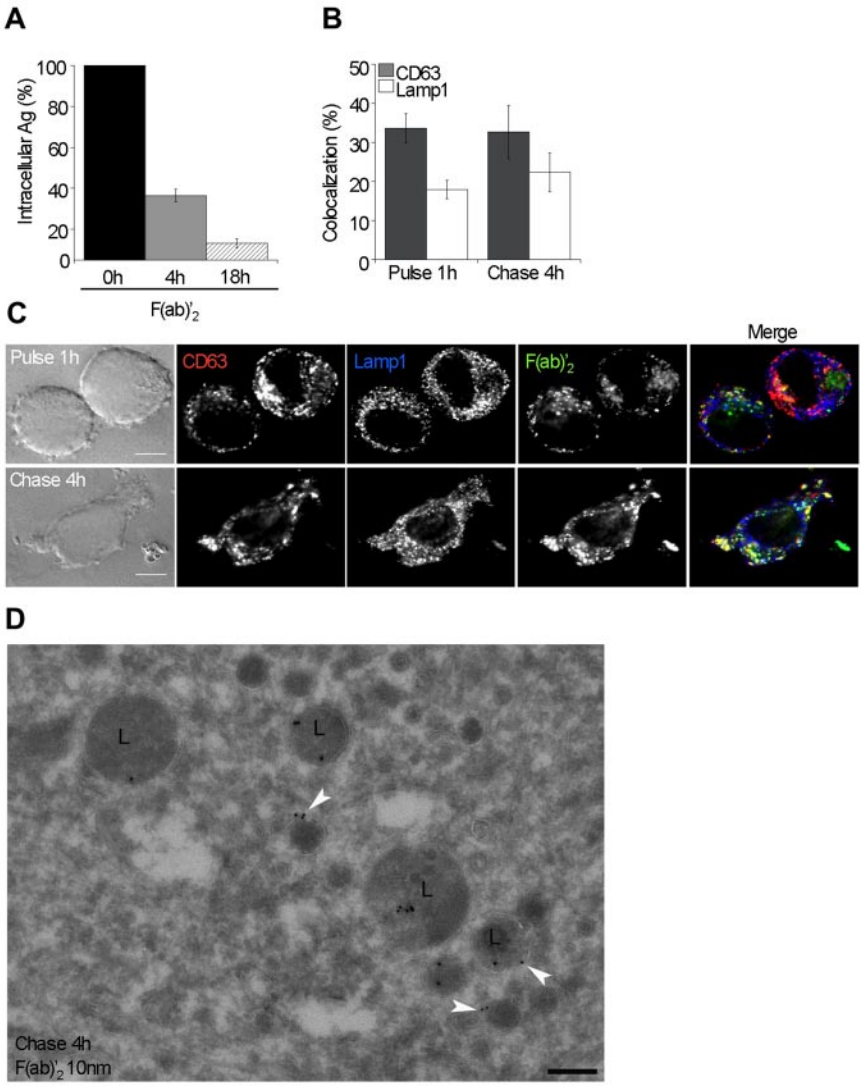

Figure 2. Immature MoDCs store macropinocytosed Ag in late endocytic compartments. (A) MoDCs were pulsed for 1 hour with 10 μg/mL of fluorescent $F(ab)'_2$ and washed and chased for 4 or 18 hours. After each time point, cells were fixed and amount of Ag was measured by flow cytometry. Results are expressed as a percentage of cells before chase. Data are mean ± SEM of 3 independent experiments. (B) MoDCs were treated as in panel A and then analyzed by wide field microscopy and deconvolution of Z-stack images. The percentage of colocalization of $F(ab)'_2$ with CD63 or Lamp1-positive compartments was measured from deconvolved images of the whole cells. Data are mean ± SEM of 3 independent experiments (20-50 cells per condition). (C) MoDCs were treated as in panel B. A medial optical section is shown. Bar represents 5 μm. (D) Immature MoDCs were pulsed for 1 hour with 50 μg/mL $F(ab)'_2$ and washed twice and chased for 4 hours before embedding for electron microscopy analysis. Immunogold labeling was performed to detect $F(ab)'_2$ on thawed cryosections (10-nm gold particles). The white arrowheads indicate label in late endosomal vacuoles; and black arrowhead, label in a tubular structure. The black arrow points to a label in a tubular extension of an early endosomal vacuole. P indicates plasma membrane; E, early endosomal vacuole; G, Golgi; M, mitochondrium; and L, late endosomal/lysosomal vacuole. Bar represents 200 nm.

measured during the assay could not account for the release detected (supplemental Figure 2B-C). Importantly, compared with other cell types, such as monocyte-derived macrophages or HeLa cells, we found that DCs have a unique ability to regurgitate undegraded Ag back to the extracellular medium (Figure 3C; supplemental Figure 2A).

Together, these results indicate that MoDCs efficiently capture and release HRP in the extracellular medium by a nonsaturable pathway that is unlikely to correspond to the classic recycling pathway.

Released native Ag can be recognized and internalized by specific B cells

To investigate uptake and subsequent delivery of unprocessed Ag by DCs, MoDCs were pulsed with 50 μg/mL of Cy2-coupled $F(ab)'_2$ anti–human IgG, which targets all surface IgG/BCR on primary human B cells, for 1 hour and then chased for 4 hours.

We first measured intracellular $F(ab)'_2$ taken up by DCs by flow cytometry and observed that, contrary to HRP, which tends to stick to the plasma membrane, $F(ab)'_2$ does not remain at the cell surface of MoDCs (Figure 3D). We then measured the release of the $F(ab)'_2$ model Ag in the supernatant of MoDCs by a dedicated ELISA test. Concentrations of $F(ab)'_2$ found in DCs supernatants were up to 12 ng/mL after a 4-hour incubation (Figure 3E). A calibration curve by flow cytometry of B cell labeled with increasing quantities of $F(ab)'_2$ showed that such an amount of Ag was enough to target 10% to 15% of primary human B cells in vitro (Figure 3F). When B cells were incubated 4 hours with the supernatant of $F(ab)'_2$-pulsed DCs, 52.1% ± 9.7% of B cells were positive for $F(ab)'_2$ compared with B cells directly incubated for 4 hours with 1 μg/mL of the $F(ab)'_2$ (Figure 3G-H). This percentage was decreased to 16.6% ± 4.6% after an overnight incubation, possibly because of Ag degradation by B cells. We checked that Ag transfer from pulsed MoDCs to B cells was not the result of cell death. Indeed, treatment of DCs with staurosporine during the chase time induced 47.7% cell death within 4 hours, but it did not improve uptake of the $F(ab)'_2$ by human B cells (supplemental Figure 2C). Importantly, we observed that only a very low percentage of B cells (2.3% ± 1%) were $F(ab)'^{+}_2$ when incubated with the supernatant of DCs fixed by PFA after the Ag pulse, indicating that active delivery of the native Ag by DCs is important for B-cell uptake (Figure 3H). In addition, when the DC supernatant was ultracentrifuged to separate the exosomal fraction from the soluble fraction,[38] we observed no transfer of $F(ab)'_2$ to the B cells with the exosomal fraction, whereas there was transfer with the supernatant devoid of exosomes, showing that the Ag is released in the soluble fraction (supplemental Figure 2D-E).

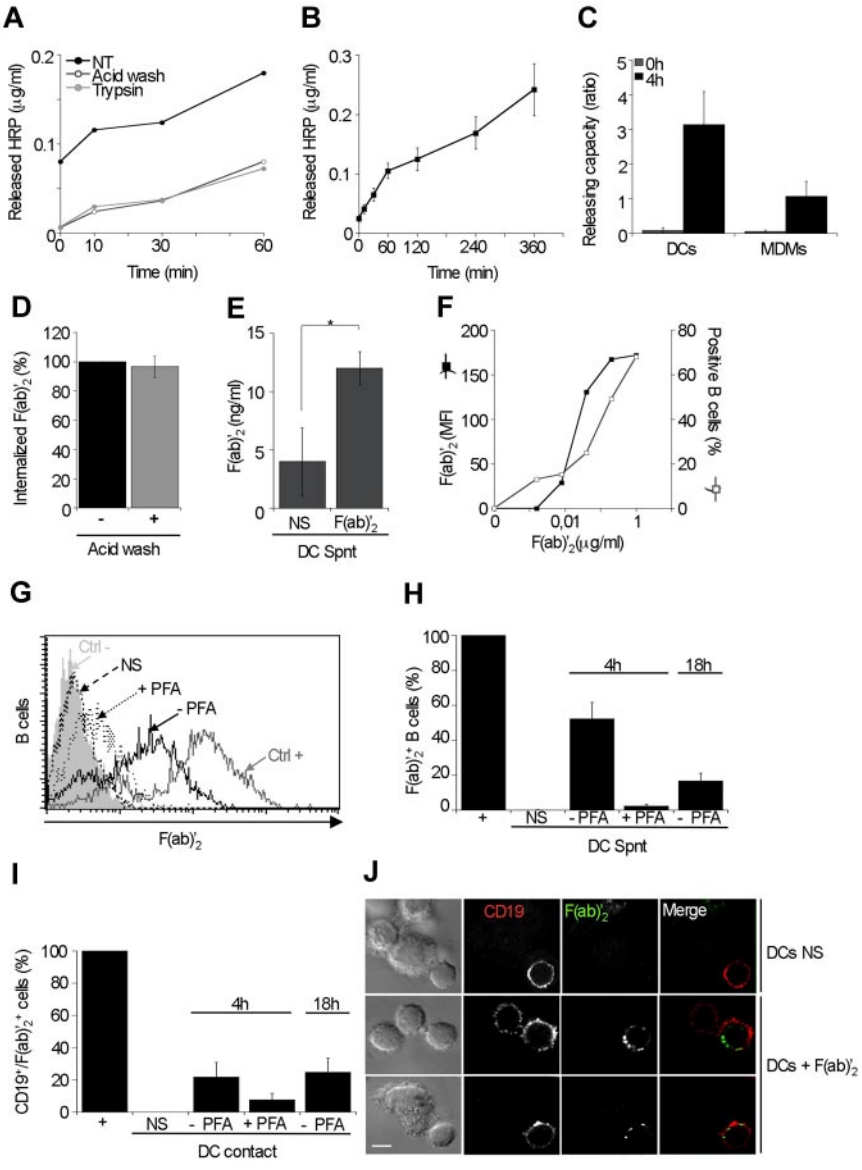

Figure 3. Immature MoDCs release part of macropinocytosed Ag under its native form and B cells capture them. (A) MoDCs were pulsed 1 hour with 1 mg/mL HRP and then washed and membrane stripped or not, either with trypsin or with acid wash. Enzymatic activity of HRP was detected in the supernatants at different time points. (B) HRP release capacity of 5 different donors was measured as in panel A during 1 hour and up to 6 hours. Data are mean ± SEM of 5 independent experiments. (C) HRP releasing capacity was measured for immature MoDCs and monocyte-derived macrophages and expressed as a ratio of HRP found inside and outside cells after 1-hour pulse and 4-hour chase. Data are mean ± SEM of 3 independent experiments. (D) DCs were pulsed for 1 hour with fluorescent F(ab)′$_2$ and then treated or not with acid wash and analyzed by flow cytometry. Data are mean ± SEM of 4 independent experiments. (E) DCs were pulsed for 1 hour with fluorescent F(ab)′$_2$ or not (NS) and then chased for 4 hours, and the F(ab)′$_2$ concentration in supernatants was measured by ELISA. (F) Primary B cells were incubated for 4 hours with increasing concentrations of fluorescent F(ab)′$_2$ and then analyzed by flow cytometry. Results are expressed both in mean fluorescence intensities and in percentage of positive B cells. (G) MoDCs were unpulsed (NS) or pulsed with 50 μg/mL of Cy2-F(ab)′$_2$ for 1 hour and then fixed with PFA (+PFA) or not (−PFA) and chased for 4 hours at 37°C. Supernatants were collected and applied to autologous primary B cells for 4 or 18 hours. As control (Ctrl+), B cells were directly incubated with 1 μg/mL of Cy2-F(ab)′$_2$ or not (Ctrl−) for 4 hours. B cells were analyzed by flow cytometry, and results are shown as a histogram. (H) MoDCs were treated as in panel G, and results are expressed as percentage of Cy2-F(ab)′2-positive B cells compared with B cells incubated directly for 4 hours with 1 μg/mL of Cy2-F(ab)′$_2$. Data are mean ± SEM of 4 independent experiments. (I) B cells were cocultured for 4 hours or 18 hours with DCs nonstimulated (NS) or pulsed with Cy2-F(ab)′$_2^+$ and fixed (+PFA) or not (−PFA) before B-cell addition. Quantifications were made with the ImageStream technology compiled with results obtained by flow cytometry. Results are expressed in percentages of CD19$^+$/F(ab)′$_2^+$ cells compared with control B cells incubated directly for 4 hours with 1 μg/mL of Cy2-F(ab)′$_2$. Data are mean ± SEM of 3 independent experiments. (J) DCs were pulsed with Cy2-F(ab)′$_2$ or not (NS) for 1 hour and then cocultured with B cells for 4 hours. Wide field fluorescent microscopy Z-stack images show B cells identified by CD19 (red) and positive for Cy2-F(ab)′$_2$ (green). Bar represents 5 μm.

We observed the same results in a nonautologous but Ag-specific system using B cells lines bearing a tetanus toxin specific BCR[39] (supplemental Figure 3A-B).

Together, these results show, with 2 different model Ag, that B cells capture and internalize nondegraded protein Ag delivered in the supernatant by pulsed DCs.

We then assessed whether this Ag delivery from DCs to B cells could be influenced by cell-cell contact. For this, MoDCs were pulsed 1 hour with 50 μg/mL of F(ab)′$_2$, washed and cocultured with autologous B cells for 4 or 18 hours. Flow cytometric analysis showed that cell-cell contact between pulsed MoDCs and B cells did not increase the amount of Ag detected in B cells after 4 or 18 hours, compared with B cells incubated with the supernatant of MoDCs (Figure 3I), although some conjugates could be observed by ImageStream technology (supplemental Figure 3C). Fluorescent microscopy on medial optical sections after deconvolution confirmed F(ab)′$_2$ staining of B cells in intracellular compartments below the CD19 surface staining (Figure 3J).

Altogether, our results show that model Ag delivered by DCs to the external medium are internalized by B cells and that DCs-B cell contact does not improve the Ag capture in vitro.

Macropinocytosed Ag is delivered to B cells from a late endosomal storage compartment in MoDCs under the control of Rab27.

We then aimed to further characterize the intracellular mechanism of Ag delivery from DCs to B cells. Thus, after a 1-hour pulse with 50 μg/mL of F(ab)′$_2$, MoDCs were treated with monensin, an inhibitor of ligand recycling and of trafficking from late endosomes to lysosomes,[40] during the 4 hours of chase at 37°C. Cells were then fixed and analyzed by flow cytometry and ImageStream technology. Monensin-treated MoDCs showed a higher amount of intracellular Cy2-coupled F(ab)′$_2$ compared with nontreated DCs after 4 hours of chase (Figure 4A-B). We also followed HRP activity in the supernatant of monensin-treated DCs and observed that DCs delivered more HRP to the external medium than nontreated control cells. This HRP release was increased with time (up to 1.7 times more than the nontreated cells; Figure 4C). This enhanced delivery was confirmed by the increased number of B cells taking up Cy2-coupled F(ab)′$_2$ from monensin-treated MoDCs compared with nontreated DCs (Figure 4D). These data show that Ag storage and delivery were improved by monensin treatment. Because

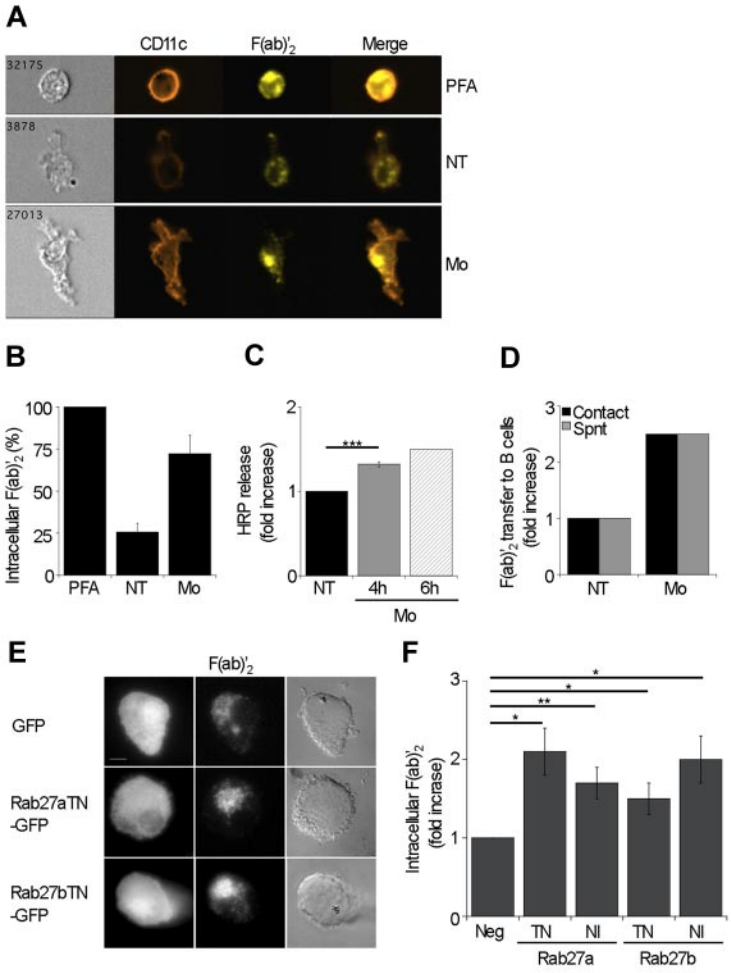

Figure 4. Extracellular release of macropinocytosed Ag occurs from late endosomes. (A) DCs were incubated with Cy2-F(ab)′$_2$ for 1 hour and then either fixed before B-cell addition (PFA) or cocultured with B cells for 4 hours in the presence of 25 μg/mL monensin (Mo) or not (NT). MoDC images were obtained with the ImageStream multispectral imaging technology. (B) DCs were treated as in panel A. Quantifications show the percentage of cell-associated F(ab)′$_2$ in MoDCs after each treatment, compared with cells fixed after 1-hour pulse. Data are mean ± SEM of 3 independent experiments. (C) DCs were incubated with HRP for 1 hour and then treated or not (NT) with monensin (Mo) during 4 and 6 hours of chase. Results are expressed as fold increase of extracellular HRP measured in monensin-treated cells compared with nontreated cells (NT) at each time point. (D) DCs were incubated with Cy2-F(ab)′$_2$ for 1 hour and then treated or not (NT) with monensin (Mo) during 4 hours of chase in the presence of B cells (contact). Supernatants were collected and applied to B cells (Spnt) for 4 hours. Cell-associated Cy2-F(ab)′$_2$ was measured by flow cytometry gated on CD19$^+$ B cells. Fold increase of efficiency of Ag transfer from DCs to B cells, from supernatants, or in cocultures in the presence of monensin were calculated compared with control (NT) conditions. Graph is representative of 2 independent experiments. (E) MoDCs were nucleofected to express GFP alone or dominant-negative form of Rab27a (Rab27aTN-GFP) or b (Rab27bTN-GFP) fused to GFP. After 6 hours, cells were pulsed with 50 μg/mL of Cy5-F(ab)′$_2$ for 1 hour, then chased for 4 hours at 37°C, and fixed and analyzed by wide field fluorescent microscopy. (F) MoDCs were nucleofected to express dominant-negative forms of Rab27a (Rab27aTN-GFP and Rab27aNI-GFP) or Rab27b (Rab27bTN-GFP and Rab27bNI-GFP) fused to GFP and then analyzed by flow cytometry to measure the quantity of intracellular Cy5-F(ab)′$_2^+$ in GFP$^+$ and GFP$^-$ cells (Neg). Results are expressed as ratio compared with Ag measured in GFP$^-$ DCs. Data are mean ± SEM of 3 independent experiments.

monensin blocks recycling from classic recycling compartments and also transport from late endosomes to lysosomes, this indicates that, under these conditions, Ag storage and delivery were enhanced because of reduction of classic recycling as well as reduction of degradation.

To get further insight into the mechanism controlling the release from a late compartment, we transiently expressed in MoDCs dominant-negative forms of Rab27, known to play a role in secretory granule and lysosome-related organelle formation.[41] Compared with transfected negative cells, MoDCs expressing dominant-negative mutants of Rab27a and Rab27b showed a higher intracellular content of F(ab)′$_2$ after a 1-hour pulse and 4-hour chase (Figure 4E-F).

These results highlight that the delivery of unprocessed Ag from a late endocytic compartment in DCs is partially controlled by Rab27.

Ag release from DCs is enhanced by the CXCL13 chemokine

We then set out to determine whether the chemokine environment could influence Ag delivery from DCs to B cells. For that, we focused on the chemokine CXCL13, which is important for B-cell homing in lymph nodes.[5,42] This chemokine has also been shown to attract a specific subset of murine DCs to B-cell follicles.[43] Surface staining and flow cytometric analysis showed that MoDCs expressed CXCR5, the receptor for CXCL13, although less than purified blood B cells, whereas Jurkat T cells were used as a control (Figure 5A-C). In addition, quantitative RT-PCR analysis showed that human and mouse DCs express CXCR5 but 150- and 189-fold less than B cells, respectively (not shown). Next, DCs were pulsed for 1 hour with 50 μg/mL of F(ab)′$_2$ and then treated with 200 ng/mL of CXCL13 during the 4 hours of chase at 37°C. Ag content of MoDCs was increased as measured by flow cytometry and ImageStream technology (Figure 5D-E). MoDCs were also pulsed with HRP and then incubated with CXCL13 or left untreated while submitted to the regurgitation assay described in Figure 3. HRP release in the extracellular medium was increased in the presence of CXCL13 compared with nontreated cells or cells treated with lipopolysaccharide (LPS; Figure 5D). Finally, we measured transfer to B cells of Ag from MoDCs pulsed with F(ab)′$_2$ and then incubated with CXCL13 or left untreated during the chase, in conditions where B cells were in contact with DCs or simply incubated with the MoDCs' supernatant (Figure 5G). We observed a slight enhancement of transfer of F(ab)′$_2$ to B cells when MoDCs were treated with the CXCL13 chemokine, whether supernatant or cell-cell contact was used.

These results show that the process of Ag delivery from DCs to B cells can be regulated by CXCL13.

B cells capture native Ag from pulsed DCs in vivo

As the mechanism of Ag delivery to B cells in lymph nodes is still unclear, we set out to determine whether B cells could capture in vivo an Ag previously internalized by DCs. For this, we purified CD11c$^+$ DCs from C57Bl/6 mice by positive magnetic selection

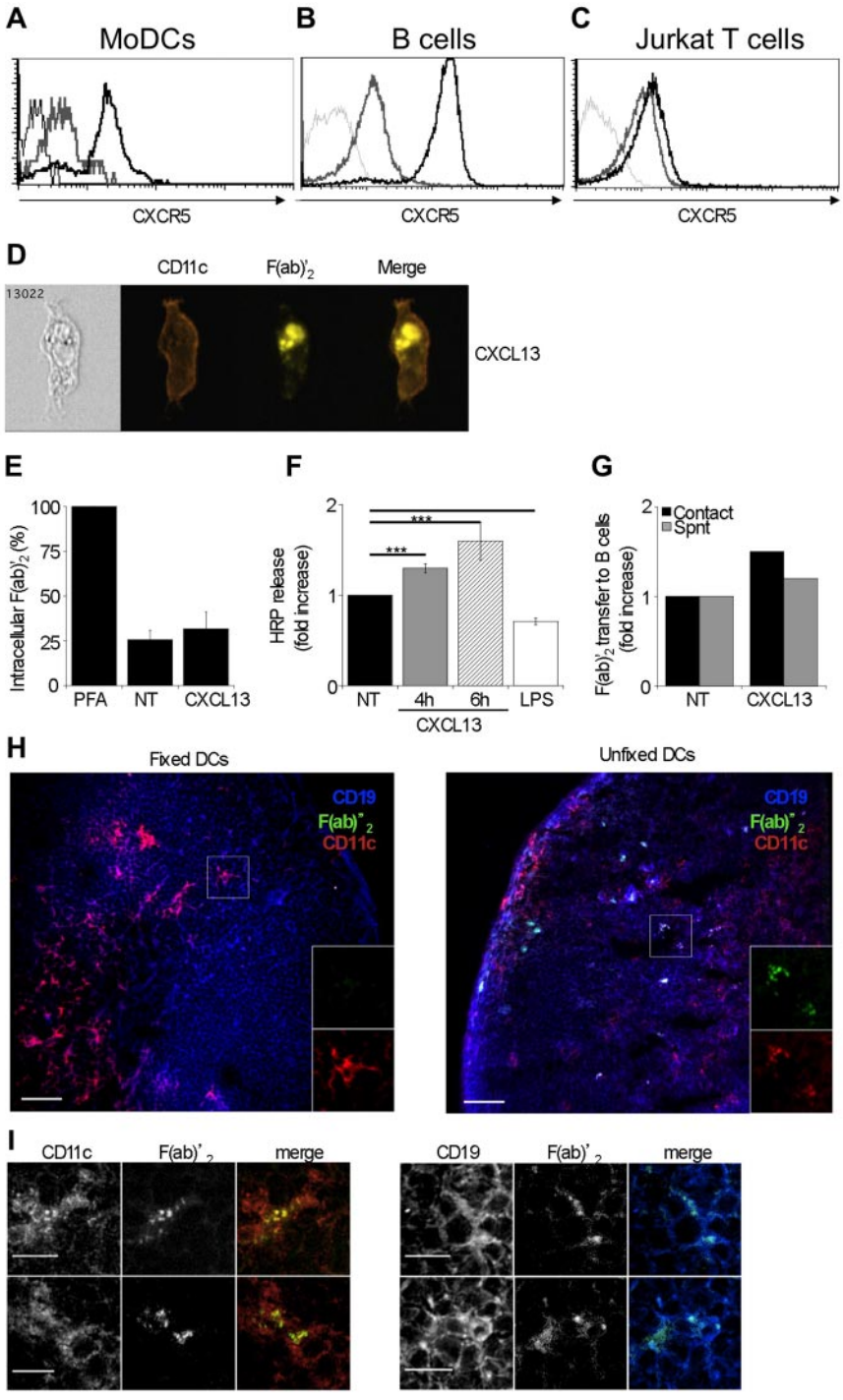

Figure 5. Ag storage and release by DCs are enhanced by CXCL13 and transfer of Ag from loaded DCs to B cells in vivo. (A-C) Flow cytometric analysis of CXCR5 staining on immature MoDCs (A), primary purified CD19$^+$ blood B cells (B), and Jurkat T cells (bold black lines) compared with isotype control (bold gray lines) and unstained cells (thin line) from the same acquisition. (D) MoDCs were pulsed with with 50 μg/mL of Cy2-F(ab)′$_2$ for 1 hour and then chased for 4 hours at 37°C in the presence of 200 ng/mL of CXCL13 and autologous B cells. Images of MoDCs obtained from ImageStream technology. (E-G) MoDCs were treated as described in Figure 4B through D, except that they were chased for 4 hours in the presence of 200 ng/mL CXCL13. (E-F) Data are mean ± SEM of 3 independent experiments. (G) Graph is representative of 2 independent experiments. (H) Purified DCs from C57Bl/6 mice were pulsed with 50 μg/mL of QDot655-coupled F(ab)′$_2$ anti–mouse IgG for 1 hour, washed twice, and fixed or not with 1% PFA for 10 minutes before footpad injections with 2.5 × 10^6 pulsed DCs. PLNs were collected after 24 hours and frozen. Immunostaining of sections was analyzed by spinning disk confocal microscopy (original magnification ×20). CD19 staining for B cells (blue), CD11c staining for DCs (red), and QDot655-coupled F(ab)′$_2$ (green) are shown. Bar represents 20 μm. Right panels: Magnified images from panel H. (I) CD11c$^+$/QDot655-coupled F(ab)′$_2^+$DCs and CD19$^+$/QDot655-coupled F(ab)′$_2^+$ B cells from the unfixed condition were observed (original magnification ×63). Bar represents 5 μm.

and pulsed them for 1 hour with 50 μg/mL of F(ab)′$_2$ anti–mouse IgG (H + L) coupled to QDot655 or 605 to target all surface BCR of B cells (see Figure 7D). Twenty-four hours after injection in the hind footpads of recipient C57Bl/6 mice, we analyzed the localization of the cells in the popliteal lymph nodes by immunofluorescence on frozen sections. In contrast to fixed DCs, nonfixed F(ab)′$_2^+$ DCs were detected on the sections and found accumulated in B cell–negative regions as well as in B cell–positive regions of the lymph node (Figure 5H-I). CD19$^+$/F(ab)′$_2^+$ B cells were detected in mice injected with nonfixed DCs (Figure 5I). The purified DCs injected into mice were a mixed population of conventional CD11c$^+$ MHCII$^+$ DCs expressing CD8α or CD11b (Figure 6A-D). CD103 was expressed by 45% of the CD8α-positive population but poorly by the CD11b-positive cells (Figure 6C-D). All subsets internalized the QDot-F(ab)′$_2$ (Figure 6E). Cells from popliteal draining lymph nodes were harvested, and CD11c$^+$ DCs and CD19$^+$ B cells were analyzed by flow cytometry for the presence of QDot-F(ab)′$_2$ (Figure 6F). Injection of CD45.2$^+$ DCs in CD45.1$^+$ animals revealed that the majority of the QDot-F(ab)′$_2$-positive DCs were of host origin (not shown). Interestingly, 97% of the DCs positive for QDot605 were CD103-positive (Figure 6G). As a control, DCs were pulsed with Ag and then fixed before injection. A higher number of CD11c$^+$/F(ab)′$_2^+$ cells were found in the lymph nodes of mice injected with nonfixed DCs compared

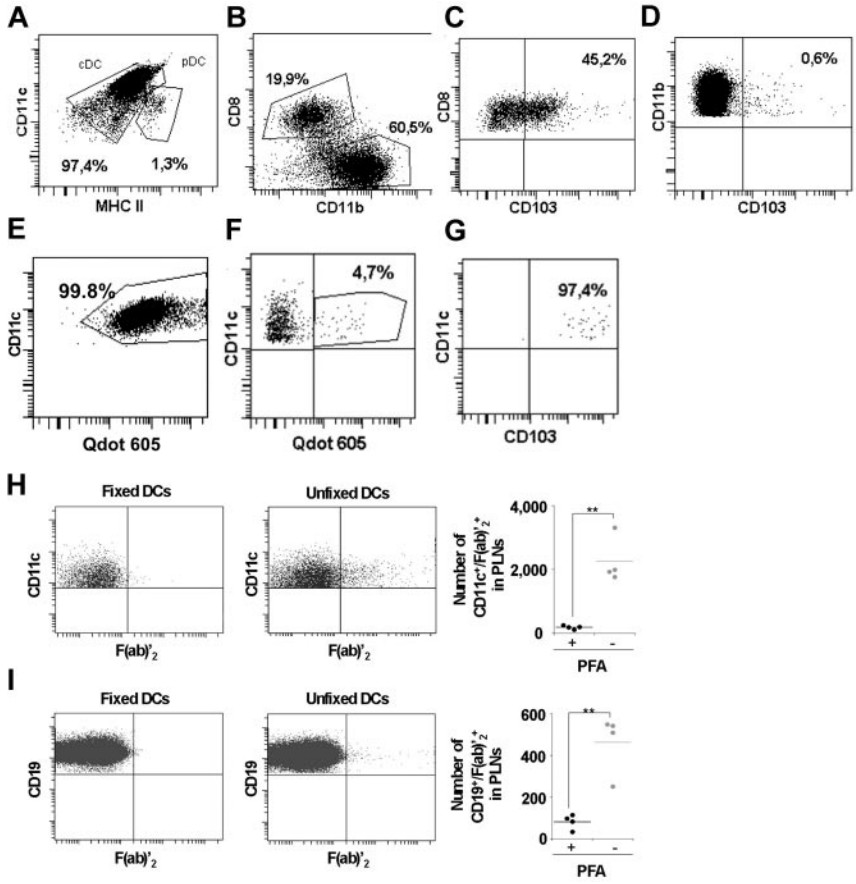

Figure 6. Flow cytometric analysis of Ag transfer from loaded DCs to B cells in vivo. (A-E) DCs purified from spleen and lymph nodes were analyzed for the expression of CD11c, MHCII, and CD317 (A). Conventional DC ($CD11c^{hi}$ MHC II $^+$) were analyzed for CD8α and CD11b expression (B). Expression of CD103 gated on cDC $CD8\alpha^+$, CD11b (C) and expression of CD103 gated on cDC $CD11b^+$ (D). Uptake of QDot605-coupled $F(ab)'_2$ anti–mouse IgG in $CD11c^+$ cells (E). (F-G) DCs purified as in panel A were pulsed with 50 μg/mL of QDot655 (H-I) or 605 (E-G)–coupled $F(ab)'_2$ anti–mouse IgG as in Figure 6. Three or 4 C57Bl/6 mice in each recipient group were injected subcutaneously into the hind footpads with 2.5×10^6 pulsed DCs. PLNs were collected after 24 hours. DCs ($CD11c^+$) and B cells ($CD19^+$) were analyzed by flow cytometry for the presence of QDot-$F(ab)'_2$ and CD103 (G), QDot-$F(ab)'_2$ (F,H-I). Quantifications show the total number of DCs and B cells positive for $F(ab)'_2$ within the collected draining PLNs.

with lymph nodes from mice injected with fixed DCs (2248 ± 716 vs 183 ± 59 cells per 2 popliteal lymph nodes; Figure 6G-H). In addition, the $CD19^+/F(ab)'_2{}^+$ population was also significantly higher in mice injected with nonfixed DCs compared with mice injected with fixed DCs (463 ± 143 vs 81 ± 35 cells per 2 popliteal lymph nodes; Figure 6H-I).

Murine B cells capture native Ag from pulsed DCs ex vivo

To better analyze the mechanism of Ag transfer, we also analyzed Ag transfer in vitro with DCs and B cells purified from mice (Figure 7). We pretreated the loaded DCs with monensin to reduce Ag recycling and/or degradation or LPS to induce maturation of the DCs for 4 hours (Figure 7). These treatments did not modify profoundly the capacity of DCs to transfer Ag to B cells, although there was a slight increase with monensin, whereas fixation of the murine DCs abrogated the transfer to B cells as already observed with human cells and in vivo.

These results show that B cells capture in vivo native Ag delivered by pulsed DCs injected in the periphery and that integrity of the DCs is required for efficient Ag delivery from injected DCs to B cells.

Discussion

In this study, we revealed that, after antigen capture by macropinocytosis, DCs have a unique capacity to store and regurgitate nonprocessed Ags, which are then taken up by B cells (Figure 7E).

We initially focused on the uptake pathway and intracellular fate of internalized Ag using human MoDCs. In these cells, macropinocytosis is completely shut down after their maturation, whereas their receptor-mediated endocytic capacities remain efficient.[44] We observed that immature MoDCs have a strong capacity to take up Ag by macropinocytosis and that this preferential pathway of uptake is independent from the biochemical nature of the Ag, as dextran, $F(ab)'_2$, HRP, or tetanus toxin proteins behave similarly. Studies using fibroblasts stimulated by growth factors have shown that macropinocytosis is dependent on PI3K and actin and is sensitive to amiloride.[18,19,20,45] This drug, widely used as a specific inhibitor of macropinocytosis, is an Na^+/H^+ ion-exchange inhibitor that was recently described to impair Rac1 and Cdc42 activity,[24] in line with the involvement of Rac and Cdc42 in macropinocytosis in murine DCs.[22,23] We also tested whether dynamin was important for macropinocytosis to proceed, as this GTPase was reported to be required for Rac1 localization and platelet-derived growth factor-induced macropinocytosis.[46] In our work, dynamin was dispensable for macropinocytosis of various cargos in human immature MoDCs. Therefore, human DCs perform efficient macropinocytosis as defined by some known molecular requirements, although the endosomes formed were of small size compared with what is described for macropinosomes in other cell types.

We then focused on the intracellular fate of macropinocytosed Ags. We showed that Ag were stored intracellularly in $CD63^+$ late endosomal compartments and partially preserved from degradation. This is in line with previous studies performed with murine DCs and various Ag.[16,26,29] We designed an assay to measure the delivery of Ag to the extracellular medium, taking advantage of the enzymatic activity of HRP. We observed a capacity for HRP release that was unique to DCs and barely exerted by macrophages and

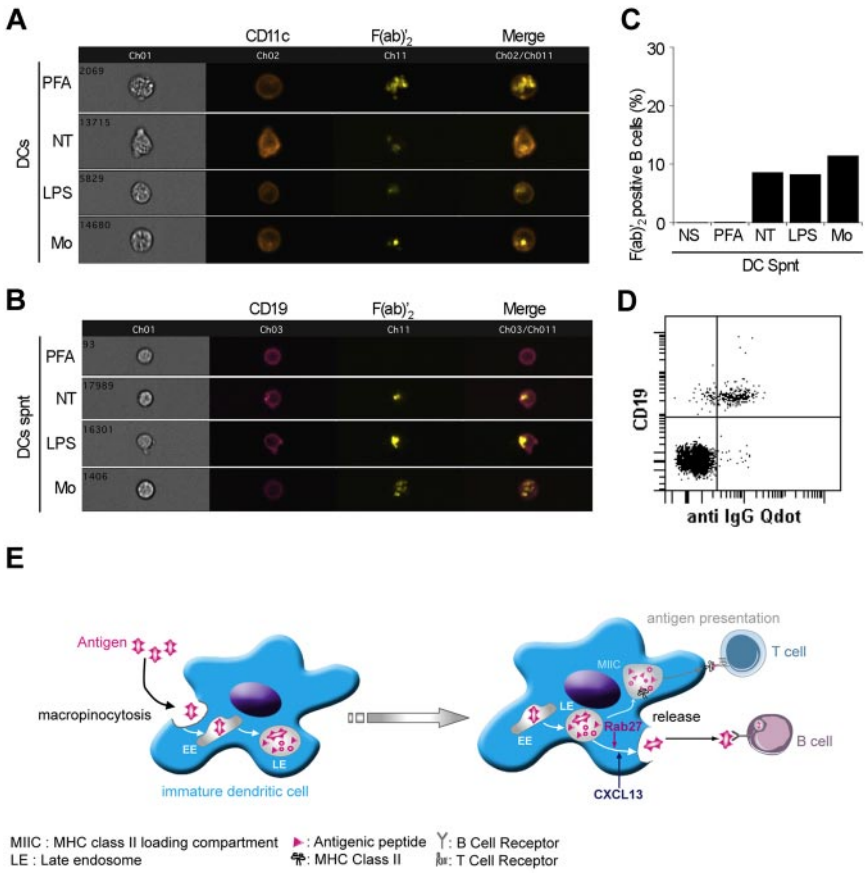

Figure 7. Murine B cells capture native Ag from pulsed DCs ex vivo. (A) CD11c$^+$ purified DCs from spleen and lymph nodes were unpulsed (NS) or pulsed with 50 μg/mL of Cy5-F(ab)′$_2$ anti–mouse IgG for 1 hour, and then fixed with PFA (+PFA) or not (NT) and chased for 4 hours at 37°C in the presence of LPS or Monensin (Mo). (B) Supernatants were collected and applied to negatively purified splenic and lymph nodes B cells for 18 hours. Cells were stained with anti–CD19 antibodies and analyzed by using ImageStream technology and FACSCalibur flow cytometry. (C) Results are expressed as number of F(ab)′$_2$-positive B cells, and the graph represents 3 independent experiments. (D) B cells negatively purified from spleen and lymph nodes were incubated with anti–CD19-PE and QDot605-F(ab)′$_2$ anti–mouse IgG antibodies to show that 81.1% of the CD19-positive B cells were labeled by the anti–mouse IgG antibodies. (E) Model of Ag capture and regurgitation by DCs to target B cells. Immature DCs efficiently capture Ag by macropinocytosis. Part of the Ag is then processed and presented to activate T cells. Part of the Ag remains undegraded and is regurgitated in the extracellular medium from late endocytic compartments under the control of Rab27. On release, Ag is captured by B cells via their BCR, and this transfer is enhanced by the CXCL13 chemokine. In vivo, Ag-loaded DCs found in the lymph node were CD103$^+$.

HeLa cells. Furthermore, the released native Ag found in DC supernatant could be recognized and internalized by specific B cells. Importantly, this uptake was not observed if DCs were fixed after Ag pulse, underlining the need for an active process in DCs to allow Ag release. Quantitative imaging flow cytometry allowed us to visualize the internalization of the released Ag by B cells and to find that cell-cell contact did not clearly improve this process in vitro. Of note, Ag transfer from DCs to B cells was enhanced when DCs were treated with monensin, a drug that blocks both the classic recycling pathway and transfer of Ag from late endosomes to lysosomes.[40] Crucially, we could not influence this Ag release by other drug treatments used to inhibit recycling, such as PdBU or primaquine (data not shown), indicating that the pathway used to deliver native macropinocytosed Ag to the external medium is clearly different from the classic recycling pathway used by transferrin, for example. This is to be compared with the exocytosis of low molecular weight dextran or inert latex beads described to occur after macropinocytosis in a calcium-dependent manner from an endocytic compartment that was not clearly defined.[47] We observed that part of the macropinocytosed Ag was stored under its native form in CD63/Lamp1-positive compartments. We found that the release was partially inhibited by negative mutants of Rab27. Rab27 controls the biogenesis of lysosome-related organelles and exocytosis of exosomes,[48] and it has been shown that exosomes of OVA-pulsed DCs bear native OVA and are able to induce anti–OVA antibody production in vivo when injected intravenously.[49] However, in our experimental conditions, the role of exosomes in Ag delivery was clearly ruled out.

We observed that the regurgitation capacity of DCs was enhanced after incubation of DCs with CXCL13. This chemokine is known to be secreted by DCs, follicular DCs, and follicular stromal cells to attract B lymphocytes.[17] Our results suggest that it might have concomitant effects on DCs themselves to synchronize the attraction of B lymphocytes with an enhanced capacity of DCs to present unprocessed Ags to them. Indeed, it has been shown in mice that a specific subset of migrating DCs (CR-Fc$^+$ DCs) localize in lymphoid follicles in response to CXCL13.[43] Therefore, our results highlight the fact that this chemokine could be crucial for efficient Ag delivery to B cells but also to follicular DCs in lymph nodes, a mechanism still unclear when the Ag is not in immune complexes. Using a model Ag that can target both IgM- and IgG-bearing B cells, we followed the migration of Ag-loaded DCs from the periphery to the draining lymph node and observed that native Ag stored by DCs was transferred to B cells, consistent with previous work performed using transgenic B cells.[7] We observed that fixed DCs were unable to promote this Ag delivery. Because fixed DCs might release antigens at the site of injection, might release debris that could have diffused, or might themselves be taken up as debris by other cell types, this experimental condition shows that the integrity of the injected DCs is needed for the transfer, suggesting that they play an active role in the transfer. Interestingly, all DC populations positive for Ag found in the lymph nodes were CD103$^+$. CD103$^+$ DCs were described to be very efficient in migration.[50] Consistent with this, we found DCs positive for the Ag in the lymph nodes that were from donor origin, although the majority of Ag-bearing DCs were of recipient origin, indicating an intermediate transfer from injected DCs to host DCs. CD103$^+$ DCs are known to be very potent for cross-presentation, but to our knowledge, this is the first time that cells positive for this marker are described in a study on B-cell antigen presentation.

Based on our results, it is tempting to propose that DC migration and Ag regurgitation provide the missing link between the periphery and B cells in lymph nodes, together with the pathways of small Ag diffusion.[5] Indeed, our work brings, for the first time, evidence for another role for the low Ag degradation capacities of DCs. In addition to providing a pool of Ag for MHC class II and class I presentation to T cells, part of this Ag can also be released under its native form in the extracellular medium to activate specific B cells. These unique capacities of DCs are certainly crucial for the very first steps of the innate and adaptive immune responses.

Acknowledgments

The authors thank Pr Jean-Pierre Kraehenbuhl for initial discussions and ideas on the project, Dr Andrés Alcover for his constant support, Dr Marie NGuyen (Imagopole, Institut Pasteur, Paris, France) for help with the ImageStream analysis, Benedicte Capron and Catherine Fabre (EFS Saint Vincent de Paul) for buffy coat supply, Drs Alain Trautmann and Emmanuel Donnadieu for discussions, antibodies, and chemokines, Pierre Bourdoncle for advice on image analysis, Maryline Favier and Corinne Lesaffre for histology sections, Franck Letourneur for help with quantitative RT-PCR, and Dr Darragh Duffy for reading the manuscript.

This work was supported by the Association pour la Recherche sur le Cancer (1105XA0830F), Fondation pour la Recherche Médicale (INE20041102865), Centre National de la Recherche Scientifique (ATIP Program), and Ville de Paris (F.N.). D.L.R. was supported by Fondation pour la Recherche Médicale, Région Ile-de-France, and Centre National de la Recherche Scientifique (postdoctoral fellowships).

Authorship

Contribution: D.L.R. designed and performed the experiments and analyzed data; A.L.B. designed, performed, and analyzed the in vivo experiments with help from K.T.; A.D. designed and performed the quantitative RT-PCR experiments; M.S. performed and analyzed the electron microscopy; R.S. and M.J. provided technical support; A.B. advised on cell biology; G.B. provided reagents and advised on immunology; F.N. designed the study; and D.L.R. and F.N. wrote the paper with comments from A.L.B., A.B., and G.B.

Conflict-of-interest disclosure: The authors declare no competing financial interests.

Correspondence: Florence Niedergang, Institut Cochin, Phagocytosis and Bacterial Invasion Group, Cell Biology and Host-Pathogen Interactions Department, 22 rue Méchain, 75014 Paris, France; e-mail: florence.niedergang@inserm.fr.

References

1. Buckwalter MR, Albert ML. Orchestration of the immune response by dendritic cells. *Curr Biol.* 2009;19(9):R355-R361.
2. Amigorena S, Savina A. Intracellular mechanisms of antigen cross presentation in dendritic cells. *Curr Opin Immunol.* 2010;22(1):109-117.
3. Gretz JE, Norbury CC, Anderson AO, Proudfoot AE, Shaw S. Lymph-borne chemokines and other low molecular weight molecules reach high endothelial venules via specialized conduits while a functional barrier limits access to the lymphocyte microenvironments in lymph node cortex. *J Exp Med.* 2000;192(10):1425-1440.
4. Roozendaal R, Mempel TR, Pitcher LA, et al. Conduits mediate transport of low-molecular-weight antigen to lymph node follicles. *Immunity.* 2009;30(2):264-276.
5. Cyster JG. B cell follicles and antigen encounters of the third kind. *Nat Immunol.* 2010;11(11):989-996.
6. Manolova V, Flace A, Bauer M, Schwarz K, Saudan P, Bachmann MF. Nanoparticles target distinct dendritic cell populations according to their size. *Eur J Immunol.* 2008;38(5):1404-1413.
7. Qi H, Egen JG, Huang AY, Germain RN. Extrafollicular activation of lymph node B cells by antigen-bearing dendritic cells. *Science.* 2006; 312(5780):1672-1676.
8. Junt T, Moseman EA, Iannacone M, et al. Subcapsular sinus macrophages in lymph nodes clear lymph-borne viruses and present them to antiviral B cells. *Nature.* 2007;450(7166):110-114.
9. Phan TG, Grigorova I, Okada T, Cyster JG. Subcapsular encounter and complement-dependent transport of immune complexes by lymph node B cells. *Nat Immunol.* 2007;8(9):992-1000.
10. Cinamon G, Zachariah MA, Lam OM, Foss FW Jr, Cyster JG. Follicular shuttling of marginal zone B cells facilitates antigen transport. *Nat Immunol.* 2008;9(1):54-62.
11. Carrasco YR, Batista FD. B cells acquire particulate antigen in a macrophage-rich area at the boundary between the follicle and the subcapsular sinus of the lymph node. *Immunity.* 2007; 27(1):160-171.
12. Batista FD, Harwood NE. The who, how and where of antigen presentation to B cells. *Nat Rev Immunol.* 2009;9(1):15-27.
13. Gonzalez SF, Degn SE, Pitcher LA, Woodruff M, Heesters BA, Carroll MC. Trafficking of B cell antigen in lymph nodes. *Annu Rev Immunol.* 2011; 29:215-233.
14. Batista FD, Iber D, Neuberger MS. B cells acquire antigen from target cells after synapse formation. *Nature.* 2001;411:489-494.
15. Suzuki K, Grigorova I, Phan TG, Kelly LM, Cyster JG. Visualizing B cell capture of cognate antigen from follicular dendritic cells. *J Exp Med.* 2009;206(7):1485-1493.
16. Wykes M, Pombo A, Jenkins C, MacPherson GG. Dendritic cells interact directly with naive B lymphocytes to transfer antigen and initiate class switching in a primary T-dependent response. *J. Immunol.* 1998;161(3):1313-1319.
17. Allen CD, Cyster JG. Follicular dendritic cell networks of primary follicles and germinal centers: phenotype and function. *Semin Immunol.* 2008; 20(1):14-25.
18. Kerr MC, Teasdale RD. Defining macropinocytosis. *Traffic.* 2009;10(4):364-371.
19. Lim JP, Gleeson PA. Macropinocytosis: an endocytic pathway for internalising large gulps. *Immunol Cell Biol.* 2011;89(8):836-843.
20. Norbury CC. Drinking a lot is good for dendritic cells. *Immunology.* 2006;117(4):443-451.
21. Mayor S, Pagano RE. Pathways of clathrin-independent endocytosis. *Nat Rev Mol Cell Biol.* 2007;8(8):603-612.
22. West MA, Prescott AR, Eskelinen EL, Ridley AJ, Watts C. Rac is required for constitutive macropinocytosis by dendritic cells but does not control its downregulation. *Curr. Biol.* 2000;10(14):839-848.
23. Garret WS, Chen LM, Kroschewski R, et al. Developmental control of endocytosis in dendritic cells by Cdc42. *Cell.* 2000;102(3):325-334.
24. Koivusalo M, Welch C, Hayashi H, et al. Amiloride inhibits macropinocytosis by lowering submembranous pH and preventing Rac1 and Cdc42 signaling. *J Cell Biol.* 2010;188(4):547-563.
25. Svensson HG, West MA, Mollahan P, Prescott AR, Zaru R, Watts C. A role for ARF6 in dendritic cell podosome formation and migration. *Eur J Immunol.* 2008;38(3):818-828.
26. Lutz MB, Rovere P, Kleijmeer MJ, et al. Intracellular routes and selective retention of antigens in mildly acidic cathepsin D/lysosome-associated membrane protein-1/MHC class II-positive vesicles in immature dendritic cells. *J. Immunol.* 1997;159(8):3707-3716.
27. Hewlett LJ, Prescott AR, Watts C. The coated pit and macropinocytic pathways serve distinct endosome populations. *J Cell Biol.* 1994;124(5): 689-703.
28. Reich M, van Swieten PF, Sommandas V, et al. Endocytosis targets exogenous material selectively to cathepsin S in live human dendritic cells, while cell-penetrating peptides mediate nonselective transport to cysteine cathepsins. *J Leukoc Biol.* 2007;81(4):990-1001.
29. Niedergang F, Sirard J-C, Tallichet Blanc C, Kraehenbuhl J-P. Entry and survival of *Salmonella typhimurium* in dendritic cells and presentation of recombinant antigens do not require macrophage-specific virulence factors. *Proc Natl Acad Sci U S A.* 2000;97(26):14650-14655.
30. Savina A, Jancic C, Hugues S, et al. NOX2 controls phagosomal pH to regulate antigen processing during crosspresentation by dendritic cells. *Cell.* 2006;126(1):205-218.
31. Delamarre L, Pack M, Chang H, Mellman I, Trombetta ES. Differential lysosomal proteolysis in antigen-presenting cells determines antigen fate. *Science.* 2005;307(5715):1630-1634.
32. van Montfoort N, Camps MG, Khan S, et al. Antigen storage compartments in mature dendritic cells facilitate prolonged cytotoxic T lymphocyte cross-priming capacity. *Proc Natl Acad Sci U S A.* 2009;106(16):6730-6735.
33. Lindquist RL, Shakhar G, Dudziak D, et al. Visualizing dendritic cell networks in vivo. *Nat Immunol.* 2004;5(12):1243-1250.
34. Martin-Fontecha A, Lanzavecchia A, Sallusto F. Dendritic cell migration to peripheral lymph nodes. *Handb Exp Pharmacol.* 2009(188):31-49.

35. Sallusto F, Cella M, Danieli C, Lanzavecchia A. Dendritic cells use macropinocytosis and the mannose receptor to concentrate macromolecules in the major histocompatibility complex class II compartment: downregulation by cytokines and bacterial products. *J Exp Med.* 1995; 182(2):389-400.
36. Hinshaw JE. Dynamin and its role in membrane fission. *Annu Rev Cell Dev Biol.* 2000;16:483-519.
37. Macia E, Ehrlich M, Massol R, Boucrot E, Brunner C, Kirchhausen T. Dynasore, a cell-permeable inhibitor of dynamin. *Dev Cell.* 2006; 10(6):839-850.
38. Thery C, Ostrowski M, Segura E. Membrane vesicles as conveyors of immune responses. *Nat Rev Immunol.* 2009;9(8):581-593.
39. Lanzavecchia A. Antigen-specific interaction between T and B cells. *Nature.* 1985;314(6011): 537-539.
40. Wileman T, Boshans RL, Schlesinger P, Stahl P. Monensin inhibits recycling of macrophage mannose-glycoprotein receptors and ligand delivery to lysosomes. *Biochem J.* 1984;220(3):665-675.
41. Seabra MC, Mules EH, Hume AN. Rab GTPases, intracellular traffic and disease. *Trends Mol Med.* 2002;8(1):23-30.
42. Ansel KM, Ngo VN, Hyman PL, et al. A chemokine-driven positive feedback loop organizes lymphoid follicles. *Nature.* 2000;406(6793):309-314.
43. Yu P, Wang Y, Chin RK, et al. B cells control the migration of a subset of dendritic cells into B cell follicles via CXC chemokine ligand 13 in a lymphotoxin-dependent fashion. *J Immunol.* 2002; 168(10):5117-5123.
44. Platt CD, Ma JK, Chalouni C, et al. Mature dendritic cells use endocytic receptors to capture and present antigens. *Proc Natl Acad Sci U S A.* 2010;107(9):4287-4292.
45. Jones AT. Macropinocytosis: searching for an endocytic identity and role in the uptake of cell penetrating peptides. *J Cell Mol Med.* 2007;11(4): 670-684.
46. Schlunck G, Damke H, Kiosses WB, et al. Modulation of Rac localization and function by dynamin. *Mol Biol Cell.* 2004;15(1):256-267.
47. Falcone S, Cocucci E, Podini P, Kirchhausen T, Clementi E, Meldolesi J. Macropinocytosis: regulated coordination of endocytic and exocytic membrane traffic events. *J Cell Sci.* 2006; 119(22):4758-4769.
48. Ostrowski M, Carmo NB, Krumeich S, et al. Rab27a and Rab27b control different steps of the exosome secretion pathway. *Nat Cell Biol.* 2010; 12(1):19-30; suppl 11-13.
49. Qazi KR, Gehrmann U, Domange Jordo E, Karlsson MC, Gabrielsson S. Antigen-loaded exosomes alone induce Th1-type memory through a B-cell-dependent mechanism. *Blood.* 2009;113(12):2673-2683.
50. del Rio ML, Bernhardt G, Rodriguez-Barbosa JI, Forster R. Development and functional specialization of CD103+ dendritic cells. *Immunol Rev.* 2010;234(1):268-281.